Quantifying the Uncertainty of Short-Term Vegetation Anomalies Detection Using Eo-Based Coarse-Resolution Vegetation Products

Zhou, Jie; Liu, Xuan; Xiong, Xuqian; Jia, Li; Lu, Jing; Cui, Yilin

DOI
10.1109/IGARSS46834.2022.9884555

Publication date
2022

Document Version
Final published version

Published in
Proceedings of the IGARSS 2022 - 2022 IEEE International Geoscience and Remote Sensing Symposium

QUANTIFYING THE UNCERTAINTY OF SHORT-TERM VEGETATION ANOMALIES DETECTION USING EO-BASED COARSE-RESOLUTION VEGETATION PRODUCTS

*Jie Zhou[1, 2, 4, *], Xuan Liu[1, 2], Xuqian Xiong[1, 2], Li Jia[3], Jing Lu[3], Yilin Cui[1, 2]*

1. School of Urban and Environmental Sciences, Central China Normal University, Wuhan, P.R. China
2. Key Laboratory for Geographical Process Analysis & Simulation of Hubei Province, Wuhan, P.R. China
3. Aerospace Information Research Institute, Chinese Academy of Sciences, Beijing, P.R. China
4. Delft University of Technology, The Netherlands

*Corresponding author: zhou.j@ccnu.edu.cn

ABSTRACT

Satellite-based Earth Observation systems archived a variety of vegetation products during the last 50 years, which can reveal regional to global ecosystem dynamics across diverse spatiotemporal scales. The anomaly metrics such as Vegetation Condition Index (VCI) defined by comparing the current vegetation growth condition to historical average status based on long-term EO-based vegetation products were widely used to delineate abnormal vegetation variation exerted by either climatic or anthropogenic factors (e.g., droughts, wildfires). However, currently available long-term vegetation products may differ from each other in terms of sensors (observational platform or spectral bands), bio-physical definitions (e.g., NDVI, EVI, LAI, and VOD), spatiotemporal resolution, as well as the time-spans, which results in inconsistency across these vegetation products. Taking the VCI as an example, this study evaluated the uncertainty of vegetation anomalies detected based on different vegetation products over the middle reach of the Yangtze River by explicitly considering the effect of sensors, biophysical definitions, and time-spans. The preliminary results showed that VCI derived from NDVI products from different sensors (AVHRR vs. MODIS) induced significant inconsistent anomalies over most landscapes. The differences resulting from products with different biophysical definitions (NDVI vs. EVI, LAI, and VOD) are much lower than those from different sensors but still significant over specific areas. As for the time-spans, the 20-year NDVI based VCI presented a considerable reduction in variance over the study area on average compared to VCI calculated based on 5-year NDVI. In summary, caution should be taken when applying EO-based vegetation products for vegetation anomalies mapping, especially for quantitative assessment.

***Index Terms*—**vegetation anomalies, uncertainty, EO-based vegetation products, Vegetation Condition Index

1. INTRODUCTION

A variety of earth observation sensors onboard satellites can capture terrestrial vegetation dynamics in regular revisit frequencies with multi-spectrum features, which can be used to derive vegetation parameters that reflect different properties of plants [1], [2]. For example, the MODIS sensors onboard both Terra and Aqua platforms observed the whole earth surface once a day since 2000 with more than 30 spectral channels [1], based on which long-term Vegetation Index (VI) and Leaf Area Index (LAI) products were freely provided for environmental and ecological applications [3]. Defined as the normalized ratio of the reflectance of red and near-infrared bands, the Normalized Difference Vegetation Index (NDVI) is a good health indicator for vegetation and has been the most popular vegetation index for vegetation monitoring and evaluation [4]. To address the saturation limitation of NDVI over densely vegetated regions, the Enhance Vegetation Index (EVI) was provided with official MODIS vegetation index products [1]. Unlike both the NDVI and EVI are unitless with unclear physical definition, the Leaf Area Index (LAI) is defined as a structure parameter for vegetation canopy with solid physical mean and is a critical parameter for earth system models [5]. Based on microwave signals, the Vegetation Optical Depth (VOD) can be retrieved to represent both the moisture and biomass dynamic inside the vegetation canopy [2]. Persistent efforts had been made to produce stable products for these vegetation parameters, and until now decades of long-term global products for each vegetation parameter had been archived and freely provided for users [6], [7]. Most of these products were provided with middle to coarse spatial resolution (>100m) and the temporal resolution from sub-daily to monthly.

Vegetation anomaly is normally evaluated by comparing the current vegetation status to the long-term historical average over the same stage of growth season [8]. The vegetation anomaly detected from long-term remote sensing vegetation products is critical for understanding the response of vegetation disturbance to climate variation (e.g., drought, wildfires) or human activity (e.g., deforestation) [9]. For example, the Vegetation Condition Index (VCI) was initially proposed to assess the evolution of large-scale drought across the North American continent, and later the VCI was generalized to monitor the health condition of vegetation by combining canopy temperature factors [10], [11]. Inconsistent spatio-temporal patterns based on the original value of vegetation parameters across different vegetation products were widely reported in previous studies [12], even products of the same vegetation parameters from different sensors (e.g., NDVI from AVHRR and MODIS). In principle, all above mentioned long-term vegetation products can be used to calculate VCI [13], [14], however, how the inconsistent patterns in original products will propagate to the detected vegetation anomaly patterns is still unknown. As a pioneer in evaluating the uncertainties of vegetation anomaly detection with remote sensing products, Meroni et al. (2019) investigated the accuracy of three commonly employed vegetation anomaly metrics (i.e., z-scores, non-exceedance probability, and vegetation condition index) concerning near real-time observations at different consolidation stages [8]. They found significant estimation errors for earlier estimates and the errors were effectively reduced in subsequent updates. Meroni et al. (2019) argued that analyzing the error structure of anomalies instead of that of the original NDVI is important because relatively minor errors in NDVI data may be amplified by the anomaly computation, especially in areas characterized by small inter-annual variability [8]. Therefore, errors that may be considered negligible for applications relying on original NDVI data may become relevant for applications using anomalies (e.g. drought detection and early warning).

In this study, the uncertainly of vegetation anomaly detection based on EO-based vegetation products was evaluated by accounting for three main factors: sensors (products of same vegetation parameters but different sensors), biophysical definitions of vegetation parameters, and time-spans of the products used to calculate historical statistics. The VCI was selected as an exemplary vegetation anomaly metric.

2. MATERIAL & METHODOLOGY

2.1 Study area

The analysis was conducted over the Middle Reach of the Yangtze River basin, which covered the Hubei, Hunan, and Jiangxi provinces of China. Both the average annual rainfall and air temperature of the study area presented as a north-to-south gradient from 830mm to more than 2500mm, and from 9 °C to 28 °C, respectively (Fig.1a and b). The cropland is mainly distributed across the low plain area, including Poyang Lake plain, Dongting Lake plain, and Jianghan Plain, which were surrounded by mountainous regions with an elevation exceeding 3000m (Fig.1c and d).

2.2 Collection of the long-term coarse resolution vegetation products and pre-processing

The EO-based vegetation products used in this study were listed in Table 1. The NDVI products (i.e., GIMMS3g) acquired from the AVHRR sensor ranged from 1981 to 2013, with a temporal resolution of 15 days and a spatial resolution of 8 km. The NDVI, EVI, and LAI products (i.e., MOD13A2, MCD15A2H) acquired from the MODIS sensor, and the NDVI and EVI products have a temporal resolution of 16 days and a spatial resolution of 1 km, and the LAI products have a temporal resolution of 8 days and a spatial resolution of 500 m, both from 2001 to 2020. The VOD Climate Archive (VODCA) have been derived from multiple sensors (SSM/I, TMI, AMSR-E, WindSat, and AMSR2) using the Land Parameter Retrieval Model, and the VOD (c-band) products ranging from 2002 to 2018 with a time resolution of 1 day and a spatial resolution of 25 km. The NDVI, EVI, and LAI products derived from optical observations are prone to atmospheric contamination. The Harmonic ANalysis of Time Series (HANTS) implemented on Google Earth Engine (GEE) platform was applied to reconstruct these products and output monthly products for vegetation anomaly calculation [15]. The daily VOD product was aggregated to a monthly scale by averaging the daily value within a month. All the products with different spatial resolutions were resampled to 1km using the bilinear interpolation method. All the products were clipped to the study area.

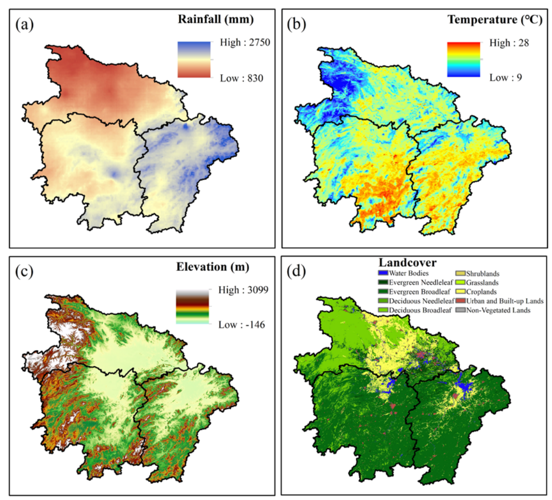

Fig 1. The geographical diagram of the Middle Reach of the Yangtze river basin. a) average annual rainfall, b) average annual air temperature, c) elevation, d) land cover type.

2.3 Calculation of discrepancies among short-term anomalies revealed by vegetation products

The VCI was used as the vegetation anomaly metric in this study. Given a monthly time series (n years) of specific vegetation parameters (VP) such as NDVI, EVI, LAI, or VOD, the VCI for an i-th month at a j-th year was calculated using equation 1.

$$VCI_{i,j}^{VP,n} = \frac{VP_{i,j} - VP_{i,min}^{n}}{VP_{i,max}^{n} - VP_{i,min}^{n}} \qquad (1)$$

Where $VP_{i,j}$ is the instantaneous observations for the i-th month at j-th year, $VP_{i,min}^{n}$ is the minimum value of the i-th month among n years, $VP_{i,max}^{n}$ is the maximum value of the i-th month among n years. n is no less than 5 and can not exceed the length of the selected vegetation products. For example, the n of VCI calculated from GIMMS3g-NDVI can reach 32.

To evaluate the impact of sensors, physical definitions, and time-spans on the VCI calculation, pixel-based VCI time series were calculated under three experimental settings listed in Table 1. Within each experimental setting, detailed product settings used for VCI calculation differed from each other by one impact factor among sensors, physical definitions, and time-spans. For example, experiment 1 is set to identify the effect from different sensors, so the vegetation parameter and time-span were kept the same.

Three metrics, i.e., correlation coefficient (R), Maximum Absolute Deviation (MAD), and Mean Bias (MB) between time series of VCI calculated based on different product settings within each experiment to quantify the discrepancy of the vegetation anomaly caused by different impact factors.

Table 1. Experimental settings for uncertainty evaluation of VCI calculation.

	Product	Sensors	VP	Time-span
Exp1	GIMMS3g	AVHRR	NDVI	2001~2013
	MOD13A2 .006	MODIS	NDVI	2001~2013
Exp2	MOD13A2	MODIS	NDVI	2003~2018
	MOD13A2	MODIS	EVI	2003~2018
	MCD15A2H	MODIS	LAI	2003~2018
	VODCA	Multi-sensors fusion	VOD (C-band)	2003~2018
Exp3	MOD13A2	MODIS	NDVI	2001~2020
	MOD13A2	MODIS	NDVI	2001~2010
	MOD13A2	MODIS	NDVI	2001~2005

3. RESULTS

According to the zonal average, the vegetation anomaly based on NDVI from different sensors (Experiment 1) revealed a significant difference and a notable increasing trend appeared in the time series of VCI based on MODIS NDVI (Fig.2a). In experiment 2, the VCIs were calculated based on different vegetation parameters (i.e., NDVI, EVI, and LAI) but all derived MODIS sensors showed quite similar temporal dynamics (Fig.2b). Again, the increasing trend was observed from the three time-series of VCIs, where the trend of NDVI derived VCI is the strongest. The VCI calculated with VOD showed minimal similar patterns with the ones from optical vegetation parameters. In experiment 3, notable differences in magnitude were observed in the VCIs calculated based on NDVI with different time-spans (Fig.2c). Specifically, the trend in VCI defined with a 20-year time-span was eliminated in the one with 5-year time-span. The study area experienced notable meteorological droughts in 2008, 2011, and 2019 according to the time series of Standard Precipitation Index (SPI) calculated based on Climate Hazards Group InfraRed Precipitation with Station data (CHIRPS) (Fig.2d). In this case, the VCI with a 5-year time-span seemed to delineate the vegetation response to drought events more reasonably.

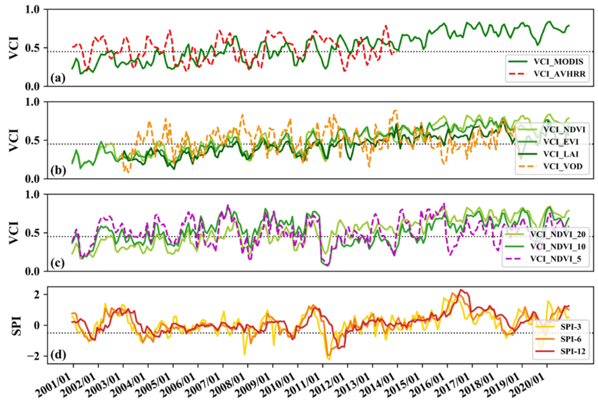

Fig.2 Time series of the regional average of SPI and VCI for different settings (2001~2020). The 20 years NDVI series were separated into four 5-year segments to construct VCI time series with a 5-year time-span in (d).

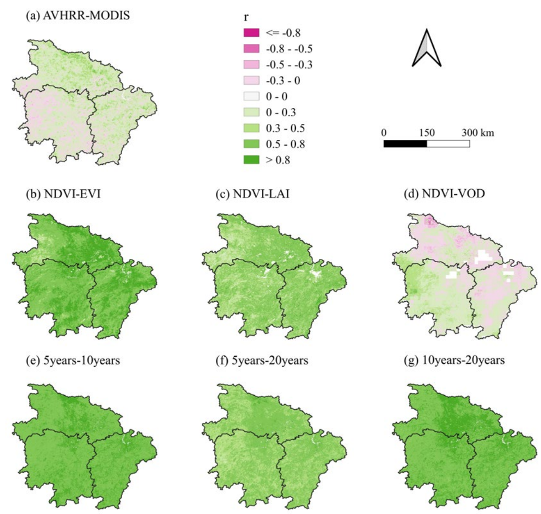

Fig.3 Pixel-based correlation of VCI calculated based on different settings

The VCIs calculated based on NDVI of MODIS and AVHRR sensors presented evident discrepancy, even negative correlation was observed in the southwestern part of the study region (Fig.3a). The MODIS-derived NDVI, EVI, and LAI products generated VCI with a very similar spatial pattern, i.e., the Pearson correlation can be larger than 0.7 over most areas (Fig.3b and c). However, the correlation over the forest area in the west seemed weaker than other places, which may be caused by the well-known saturation issues of NDVI over densely vegetated regions. The relationship between vegetation anomaly signals detected using NDVI and VOD products showed quite diverse spatial patterns, where the southwestern area was dominated by positive correlation while other area was dominated by negative correlation (Fig.3d). The correlation coefficient among VCI based on MODIS NDVI with different time-spans was larger than 0.5 over most areas, which implied that time-span difference imposed a smaller impact on VCI calculation compared to sensor difference and vegetation parameter difference.

4. DISCUSSION & CONCLUSION

The remote sensing-based vegetation anomaly metrics such as VCI are critical for large-scale vegetation health or disturbance assessment. Moreover, the VCI had been widely used for drought monitoring by combing with another thermal index such as Temperature Condition Index (TCI). The VCI calculated based on diverse vegetation products may produce large uncertainty in final vegetation assessment results, which had never been carefully quantified. This study investigated the uncertainty of VCI calculation in terms of sensors, vegetation parameters, as well as time-spans. The sensor difference resulted in a large discrepancy in VCI calculation, which further highlights the inconsistency between GIMMS3g NDVI and MODIS NDVI products [16]. The different VP products (even from the same sensor) produced significant differences in VCI over a specific area that can be attributed to the physical definition difference of the parameters. For example, the VCI derived from VOD even revealed a contrast pattern with the one derived from NDVI, which can be explained that the VOD mainly contained information of vegetation moisture content while the NDVI is a general proxy of vegetation greenness [2]. The uncertainty caused by the time-span difference seems much smaller but still significant for some areas. Moreover, the long-term trend in the vegetation products may result in large uncertainty in detected short-term vegetation anomalies, which may cause inaccurate vegetation assessment results (e.g. drought monitoring). In summary, the uncertainty of vegetation anomaly induced by EO-based vegetation products should be carefully evaluated before further application.

5. ACKNOWLEDGE

The study was financially funded by the National Natural Science Foundation of China (No. 42171371).

6. REFERENCES

[1] A. Huete, K. Didan, T. Miura, E. P. Rodriguez, X. Gao, and L. G. Ferreira, "Overview of the radiometric and biophysical performance of the MODIS vegetation indices," Remote Sensing of Environment, vol. 83, no. 1, pp. 195–213, Nov. 2002.

[2] L. Moesinger et al., "The global long-term microwave Vegetation Optical Depth Climate Archive (VODCA)," Earth System Science Data, vol. 12, no. 1, pp. 177–196, Jan. 2020.

[3] Y. Tian et al., "Multiscale analysis and validation of the MODIS LAI product: I. Uncertainty assessment," Remote Sensing of Environment, vol. 83, no. 3, pp. 414–430, Dec. 2002.

[4] C. J. Tucker, "Red and photographic infrared linear combinations for monitoring vegetation," Remote Sensing of Environment, vol. 8, no. 2, pp. 127–150, May 1979.

[5] Y. Knyazikhin, J. V. Martonchik, R. B. Myneni, D. J. Diner, and S. W. Running, "Synergistic algorithm for estimating vegetation canopy leaf area index and fraction of absorbed photosynthetically active radiation from MODIS and MISR data," Journal of Geophysical Research: Atmospheres, vol. 103, no. D24, pp. 32257–32275, 1998.

[6] J. E. Pinzon and C. J. Tucker, "A Non-Stationary 1981–2012 AVHRR NDVI3g Time Series," Remote Sensing, vol. 6, no. 8, Art. no. 8, Aug. 2014.

[7] Y. Bai, Y. Yang, and H. Jiang, "Intercomparison of AVHRR GIMMS3g, Terra MODIS, and SPOT-VGT NDVI Products over the Mongolian Plateau," Remote Sensing, vol. 11, no. 17, Art. no. 17, Jan. 2019.

[8] M. Meroni, D. Fasbender, F. Rembold, C. Atzberger, and A. Klisch, "Near real-time vegetation anomaly detection with MODIS NDVI: Timeliness vs. accuracy and effect of anomaly computation options," Remote Sensing of Environment, vol. 221, pp. 508–521, Feb. 2019.

[9] N. Nicolai-Shaw, J. Zscheischler, M. Hirschi, L. Gudmundsson, and S. I. Seneviratne, "A drought event composite analysis using satellite remote-sensing based soil moisture," Remote Sensing of Environment, vol. 203, pp. 216–225, Dec. 2017.

[10] F. N. Kogan, "Remote sensing of weather impacts on vegetation in non-homogeneous areas," International Journal of Remote Sensing, vol. 11, no. 8, pp. 1405–1419, Aug. 1990.

[11] F. N. Kogan, "Global Drought Watch from Space," Bulletin of the American Meteorological Society, vol. 78, no. 4, pp. 621–636, Apr. 1997.

[12] Z. Xiao, S. Liang, and B. Jiang, "Evaluation of four long time-series global leaf area index products," Agricultural and Forest Meteorology, vol. 246, pp. 218–230, Nov. 2017.

[13] M. H. Afshar, A. Al-Yaari, and M. T. Yilmaz, "Comparative Evaluation of Microwave L-Band VOD and Optical NDVI for Agriculture Drought Detection over Central Europe," Remote Sensing, vol. 13, no. 7, Art. no. 7, Jan. 2021.

[14] H. de Sanchez and A. Luisa, "Vegetation Optical Depth: its potential as an agricultural drought indicator: A case study on pepper fields in Indonesia," 2018, Accessed: Dec. 22, 2021.

[15] J. Zhou, L. Jia, and M. Menenti, "Reconstruction of global MODIS NDVI time series: Performance of Harmonic ANalysis of Time Series (HANTS)," Remote Sensing of Environment, vol. 163, pp. 217–228, Jun. 2015.

[16] R. Fensholt and S. R. Proud, "Evaluation of Earth Observation based global long term vegetation trends — Comparing GIMMS and MODIS global NDVI time series," Remote Sensing of Environment, vol. 119, pp. 131–147, Apr. 2012.